environmental sciences proceedings

MDPI

Proceeding Paper

Time Series Analysis of Sea Ice Production in Polynyas in Amery Ice Shelf Region of Antarctica

Miao Gu *

College of Surveying and Geo-Informatics, Tongji University, Shanghai 200092, China

* Correspondence: gumiao_edu@163.com

† Presented at the 5th International Electronic Conference on Remote Sensing, 7–21 November 2023; Available online: https://ecrs2023.sciforum.net/.

Abstract: Amery Ice Shelf region is a major source of sea ice production which is linked to global climate. In 2019, there is a collapse event occurred in Amery Ice Shelf region and sea ice production before and during the collapse event needs to be studied. In this study, polynyas in Amery ice shelf region are extracted according to ice thickness and sea ice production is obtained by calculating heat flux during winter time (March-October) in 2013-2020. It is found that sea ice production of polynyas fluctuates greatly and the maximum annual ice production occurred in 2018 which is up to 225.4 km^3. As for collapse event in 2019, it is assumed that the collapse event may have exacerbated the volatility and instability of sea ice production.

Keywords: Polynya; sea ice production; Amery ice shelf

1. Introduction

Antarctic coastal polynyas are open water or thin ice regions formed by the divergent ice motion because of offshore winds or oceanic currents, they usually appear regularly in the same locations in winter [1]. Due to the poor heat insulation property of thin ice in winter, intensive heat loss towards atmosphere occurs in Antarctic coastal polynya areas and leads to the formation of plenty of sea ice [2]. Antarctic coastal polynyas are important producers of sea ice, and about 10% of sea ice in Southern Ocean is produced from Antarctic coastal polynyas [3]. When a large amount of sea ice is produced in the Antarctic coastal polynyas, salt originally in the seawater which later frozen into sea ice is precipitated and then dissolves in the surrounding seawater to form a very dense brine, the brine is a major source of the world's densest water whose name is Antarctic bottom water (AABW) [4,5]. Therefore, studying the variability of the time series of sea ice production (SIP) of Antarctic coastal polynyas helps to better estimate the associated AABW production. Recent studies have found that polynyas in the Amery Ice Shelf region which is located on the East Antarctic coast, are major source areas of SIP and AABW production in Antarctica [6,7]. What's more, between 20 and 25 September 2019, the Amery Ice Shelf collapsed, with an area of 1,636 km^2 of disintegration, which is roughly twice the size of New York City. As a result of the collapse event, the large iceberg D28 broke away from the Antarctic continent and slid into the ocean. There is a great need to study SIP in the Amery Ice Shelf region during the collapse event and in the years preceding it.

For the purpose of SIP calculations, the most widely used method is based on heat flux. Assuming that all heat flux lost from the surface of the polynya is used for ice production, the heat loss from the surface of the polynya is calculated based on reanalysis of the meteorological data, and SIP can subsequently be calculated from the heat loss as a function of ice production. In order to implement the heat flux-based calculation of SIP from polynyas, two key steps are required: polynya extraction and heat loss calculation. As for polynya extraction, passive microwave is widely used to retrieve thin ice thickness

Citation: To be added by editorial staff during production.

Academic Editor: Firstname Lastname

Published: date

(SIT) and then polynyas are extracted according to the threshold of SIT [6,8,9]. In terms of heat loss calculations, it is found that heat loss consists of four parts, including shortwave radiative heat flux, net longwave radiative heat flux, latent heat flux and sensible heat flux [3,6]. Methods for calculating these heat fluxes in the Antarctic coastal sea ice and open water regions are summarized [10].

In this paper, the time-series variation of SIP in polynyas in the Amery Ice Shelf region from 2013 to 2020 is analyzed and impact of the ice shelf collapse event on SIP are assumed.

2. Methods

2.1. Extracion of Polynyas

The key to the extraction of polynyas is retrieving SIT. Thin ice (SIT ≤ 0.2m), thick ice and seawater have large differences in passive microwave brightness temperatures (TBs) due to differences in physical properties (e.g., surface salinity, surface temperature, dielectric properties) [11,12]. In this paper, Advanced Microwave Scanning Radiometer 2 (AMSR2) Level3 monthly TBs data with gird size of 10km×10km provided by Japan Aerospace Exploration Agency (JAXA) is used for retrieving SIT. TBs at 36.5 GHz and 89 GHz are used because they can obtain the salinity information of sea ice surface which is highly correlated with SIT of thin ice. It is found that there is a negative correlation between polarization ratio (PR) of TBs and SIT of thin ice [6,8] and PR can be calculated by equation 1. Based on the relationship, SIT of thin ice can be calculated with an empirical equation shown in equation 2-3 [8].

$$PR = (TBs(V) - TBs(H)) / (TBs(V) + TBs(H)) \quad (1)$$

$$h(89) = \exp(1 / (104\ PR(89) - 0.07)) - 1.07 \quad (2)$$

$$h(36) = \exp(1 / (72\ PR(36))) - 1.08 \quad (3)$$

Where PR(89) and PR(36) represent PR at 89 GHz and 36.5 GHz respectively, and H and V represent horizontal polarization and vertical polarization respectively. If the PR(89) ≥ 0.062 for a particular pixel, the corresponding SIT is considered to be 0-0.1 m and is calculated using equation 2 above. If PR(36) of a certain pixel satisfies $0.057 < PR(36) \leqslant 0.083$, the SIT of the pixel is regarded as 0.1-0.2 m, and is calculated using equation 3 above. All the sea ice with SIT less than 0.2m are extracted as polynyas.

After extracting polynyas, fast ice needs to be extracted, as fast ice and thin ice of polynyas have similar physical properties and fast ice are often misclassified as polynyas [6]. In this paper, gridded Antarctic fast ice extend on a weekly basis from 2013 to 2020 with gird size of 10km×10km provided by National Snow and Ice Data Center (NSIDC) is used.

2.2. Calculation of Sea Ice Production

It is assumed that all the heat loss from polynya to atmosphere is devoted to sea water freezing [8]. The key to calculating SIP is to calculate heat loss *Q*, including shortwave radiative heat flux *S*, net longwave radiative heat flux *L*, latent heat flux *Fe* and sensible heat flux *Fs*.

$$Q = S + L + Fs + Fe \quad (4)$$

All of the four types of heat flux can be obtained from fifth-generation atmospheric reanalysis of the global climate (ERA5) released by European Centre for Medium-Range Weather Forecasts (ECMWF) [13].

The SIP can then be calculated pixel by pixel according to the following equation:

$$SIP = Q/(\rho_i L_f) \quad (5)$$

where ρ_i is the sea ice density, which is taken as 920 kg • m^{-3}. L_f is the latent heat of melting of the sea ice, and L_f is taken to be 0.334 MJ • kg^{-1} according to previous study [8].

Using the above procedure, SIP of each pixel in the corresponding period can be obtained, and its spatial accumulation can be used to obtain the total SIP in the polynya.

3. Results and Discussion

Two polynyas in the Amery Ice Shelf region are extracted: Cape Darnley polynya (CDP) and Mackenzie Bay polynya (MBP). Subsequently, the area and SIP of CDP and MBP are calculated separately, and the time series of the polynya area and SIP are analyzed.

3.1. Analysis of Polynya Area

3.1.1. Accuracy Assessment of Polynya Area

In order to verify the accuracy of polynya extraction, polynyas' region is extracted by means of multiscale segmentation from high-resolution Sentinel-1 images and it is used as a reference for comparison. Taking 20 September 2015 as an example, the extent of polynyas extracted based on Sentinel-1 image and AMSR2 image are shown in Figure 1. The two high backscatter areas marked by the red line in Figure 1 (a) are polynyas, the larger polynya extend in the northern part of the bias is CDP, and the other is MBP. The low backscatter areas in the middle of the two polynyas and along the shoreline of the western side of the CDP are fast ice. Comparison of the two figures shows that the locations and ranges of polynyas extracted by the two data source are basically consistent. Then, a quantitative comparison can determine that AMSR2 extracts polynyas with a certain degree of accuracy, as shown in Table 1.

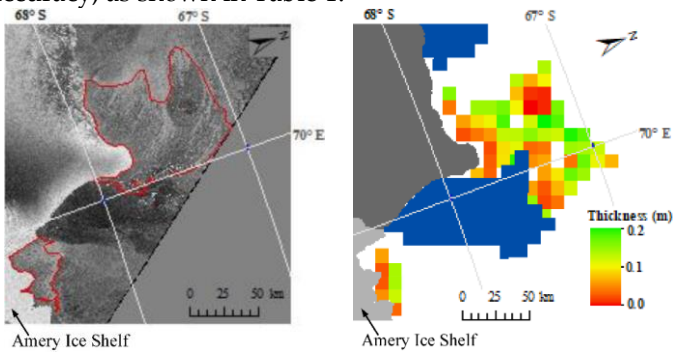

Figure 1. Comparison of extracted polynyas in 20 September 2015 based on (**a**) Sentinel 1 and (**b**) AMSR2.

Table 1. Comparison of the results of extracted polynya area based on Sentinel 1 and AMSR2.

	Area of CDP (km²)	**Area of MBP (km²)**
Based on Sentinel 1	6203	979
Based on AMSR2	6400	900
Difference	197	79
Proportion of the Difference	3.2%	8.1%

3.1.2. Time Series Analysis of Polynya Area

Annual mean polynya area is calculated by averaging monthly data, and then the interannual change of the annual mean polynya area from 2013 to 2020 is analyzed, and the corresponding change graph is shown in Figure 2.

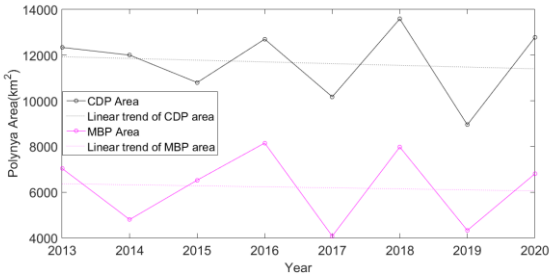

Figure 2. Interannual variability of annual mean area of polynyas in the Amery Ice Shelf region.

Overall trends show that both polynya areas are trending downward with small fluctuations, and that CDP and MBP have had relatively consistent trends over the 2013-2020 period, with the exception of 2014-2015 when CDP is trending downward but MBP is trending upward. All other years have maintained relatively consistent increasing and decreasing trends. Both CDP and MBP show large fluctuations. The year with the largest annual mean area of CDP was 2018, which had an annual mean area of 13,588 km², and the smallest annual mean area of CDP occurred in 2019, which was about 9,850 km²; the year with the largest annual mean area of MBP was 2016, which had an area of 8150 km², and the smallest annual mean area of MBP occurred in 2017, which was about 4075 km².

3.2. Analysis of Sea Ice Production in Polynyas

3.2.1. Accuracy Assessment of Sea Ice Production in Polynyas

The key to the calculation of SIP is the extraction of the polynya area, and the calculation of heat loss already has more mature products (such as ERA5, etc.), so the error in the calculation of SIP in this paper mainly comes from the extraction of the polynya area. According to the comparison with SAR images in Figure 1, the extraction of polynyas based on AMSR2 in this paper has a certain accuracy, in addition, the ERA5 reanalysis of meteorological data used in this paper is also a relatively reliable data product, so the accuracy of the calculation of SIP in this paper has a certain guarantee.

3.2.2. Spatial Distribution of SIP in Polynyas

Annual mean SIP in the Amery Ice Shelf region is calculated and the spatial distribution of SIP was mapped, as shown in Figure 3. In the CDP region, SIP is higher in the area near the eastern fast ice and shelf and in the central area, while SIP is lower in the relatively outlying areas to the west and north. In the MBP region, SIP is higher in areas close to the Amery Ice Shelf and lower in areas to the north and east.

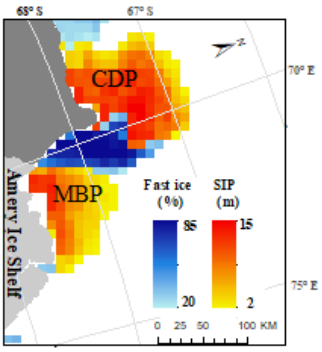

Figure 3. Spatial distribution of mean annual ice production in polynyas in Amery Ice Shelf region.

3.2.3. Time Series Analysis of Sea Ice Production in Polynyas

The annual SIP of CDP and MBP have a relatively consistent trend and are also in high agreement with the trend in area. Overall, the annual SIP of the two polynyas fluctuates widely, with the overall trend of SIP fluctuating downward in the CDP and fluctuating upward in the MBP. SIP in CDP is generally larger than that in MBP, with its highest SIP occurring in 2018, when its SIP was up to 137.5 km^3, and its lowest SIP occurring in 2019, when SIP was about 87.6 km^3. MBP's highest SIP was about 87.9 km^3 in 2018 and its lowest SIP was 45.9 km^3 in 2014. Both CDP and MBP reached a maximum SIP in 2018.

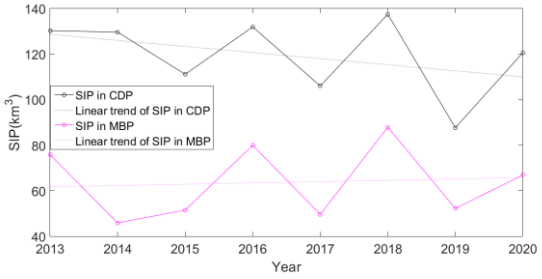

Figure 4. Interannual variability of annual SIP of polynyas in the Amery Ice Shelf region.

Multi-year average SIP in each month in CDP and MBP are shown in Figure 5. Both CDP and MBP have their intra-year maximum in March, and variances of their SIP are largest in March. CDP has a general trend of slowly decreasing trend, with the highest ice production in March, a slow increase in April-June, a decrease in July, a secondary peak in August, and then a slow decrease again in August-October. MBP, on the other hand, is on a continuous downward trend, with a larger decline in March-May and a smaller decline in June-October.

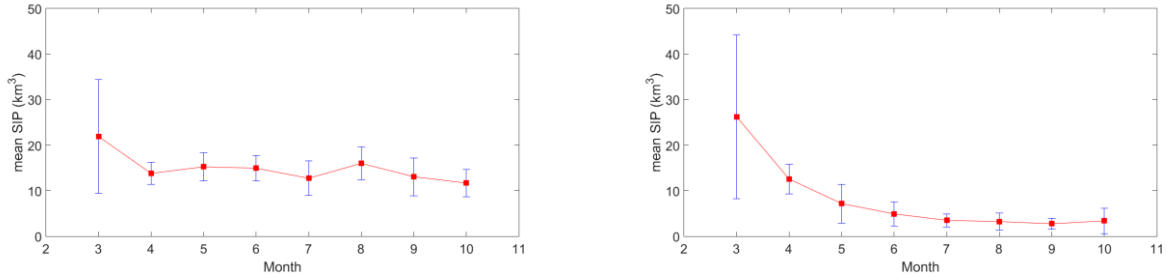

(**a**) (**b**)

Figure 5. Multi-year average SIP in each month in (**a**) CDP and (**b**) MBP.

3.3. Impact of Collapse Event on Sea Ice Production

Due to the collapse event of the Amery Ice Shelf from 20-25 September 2019, the daily SIP from 1 September to 10 October 2019 is calculated and analyzed. Time series of daily SIP is shown in Figure 6. The daily SIP of both polynyas before and after collapse showed a fluctuating downward trend, and before the collapse event, the SIP of CDP was fluctuating downward and fluctuating with a large amplitude, while MBP was firstly increasing and then decreasing. After the collapse, the daily SIP of the CDP decreased to 0.10 km^3 and then increased quickly, while the daily SIP of MBP experienced a 'down, up, down' trend. It can be assumed that the collapse event may have exacerbated the volatility of the SIP changes.

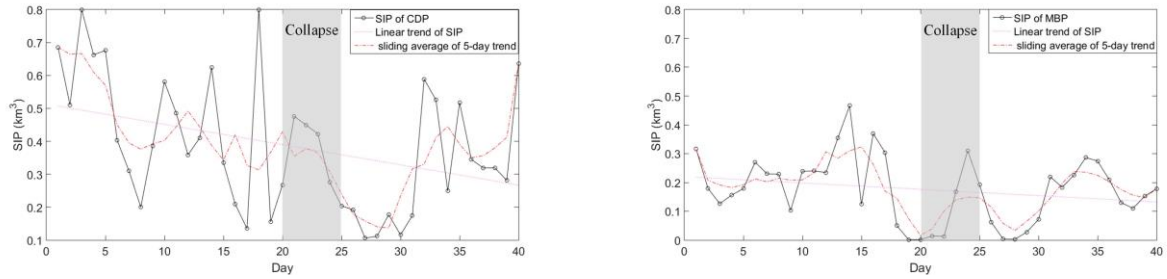

(**a**) (**b**)

Figure 6. Figure of daily SIP from 1 September to 10 October 2019 in (**a**) CDP and (**b**) MBP.

4. Conclusions

In this paper, polynyas in the Amery Ice Shelf region are extracted and SIP is calculated for 2013-2020. It is found that both polynyas in the Amery Ice Shelf region have large fluctuations in the time series of area and SIP, with the maximum intra-annual SIP occurring frequently in March. In addition, based on the analysis of SIP before and after the collapse event, it is assumed that the collapse event may have increased the volatility of SIP.

References

1. Morales Maqueda, M. A.; Willmott, A. J.; Biggs, N. R. T. Polynya Dynamics: a Review of Observations and Modeling[J]. Reviews of Geophysics.2004,42(1).
2. Maykut, G. A. Energy exchange over young sea ice in the central Arctic[J]. Journal of Geophysical Research: Oceans, 1978, 83(C7): 3646-3658.
3. Tamura, T.; Ohshima, K. I.; Nihashi, S. Mapping of sea ice production for Antarctic coastal polynyas[J]. Geophysical Research Letters. 2008, 35(7):284-298.
4. Gordon, A. L.; Orsi, A. H.; Muench, R.; et al. Western Ross Sea continental slope gravity currents[J]. Deep Sea Research Part II: Topical Studies in Oceanography, 2009, 56(13-14): 796-817.
5. Mensah, V.; Nakayama, Y.; Fujii, M.; et al. Dense water downslope flow and AABW production in a numerical model: Sensitivity to horizontal and vertical resolution in the region off Cape Darnley polynya[J]. Ocean Modelling, 2021, 165: 101843.
6. Nihashi, S.; Ohshima, K. I. Circumpolar Mapping of Antarctic Coastal Polynyas and Landfast Sea Ice: Relationship and Variability[J]. Journal of Climate.2015,28(9):3650-3670.
7. Ohshima, K. I.; Fukamachi, Y.; Williams, G. D.; et al. Antarctic Bottom Water production by intense sea-ice formation in the Cape Darnley polynya[J]. Nature Geoscience, 2013, 6(3): 235-240.
8. Nihashi, S.; Ohshima, K. I.; Tamura, T. Sea-Ice Production in Antarctic Coastal Polynyas Estimated From AMSR2 Data and Its Validation Using AMSR-E and SSM/I-SSMIS Data[J]. IEEE Journal of Selected Topics in Applied Earth Observations and Remote Sensing.2017,10(9):3912-3922.
9. Ohshima, K. I.; Nihashi, S.; Iwamoto, K. Global view of sea-ice production in polynyas and its linkage to dense/bottom water formation[J]. Geoscience Letters.2016,3(1):13.
10. Nihashi, S.; Ohshima, K. I. Relationship between ice decay and solar heating through open water in the Antarctic sea ice zone[J]. Journal of Geophysical Research: Oceans.2001,106(C8):16767-16782.
11. Cox, G. F. N.; Weeks, W. F. Salinity variations in sea ice[J]. Journal of Glaciology, 1974, 13(67): 109-120.
12. Kalnay, E.; Kanamitsu, M.; Kistler, R.; et al. The NCEP/NCAR 40-year reanalysis project[J]. Bulletin of the American meteorological Society, 1996, 77(3): 437-472.
13. Hersbach, H.; Bell, B.; Berrisford, P.; et al. ERA5 hourly data on single levels from 1959 to present [Dataset]. Copernicus Climate Change Service (C3S) Climate Data Store (CDS)[J]. 2018.
14.